

Conditions for Saddle-Node Bifurcations in AC/DC Power Systems

Claudio A. Cañizares

University of Waterloo

Department of Electrical and Computer Engineering

Waterloo, Ontario N2L 3G1

Canada

Saddle-node bifurcations are dynamic instabilities of differential equation models that have been associated with voltage collapse problems in power systems. This paper presents the conditions needed for detecting these types of bifurcations using power flow equations for a dynamic model of ac/dc systems, represented by differential equations and algebraic constraints. Two methods typically used to detect saddle-node bifurcations, namely, direct and parameterized continuation methods, are briefly analyzed from the point of view of numerical robustness.

Keywords: saddle-node bifurcations, voltage stability, ac/dc power systems, numerical robustness

I. Introduction

Hopf bifurcations and saddle-node bifurcations, or turning points, have been recognized as some of the reasons, albeit not the only ones, for voltage stability problems in a variety of power system models^{1–8}. Local bifurcations are detected by monitoring the eigenvalues of the current operating point. As certain parameters in the system change slowly, allowing the system to quickly recover and maintain a stable operating point, the system eventually turns unstable, either due to one of the eigenvalues becoming zero (saddle-node, transcritical, pitchfork bifurcations), or due to a pair of complex conjugate eigenvalues crossing the imaginary axes of the complex plane (Hopf bifurcation). The instability of the system is reflected on the state variables, usually represented by frequency, angles and voltages, by an oscillatory behavior or a continuous change. For a PQ load model these bifurcations can be associated to the power transfer limit of the transmission system⁸; in other instances the bifurcations appear due to voltage control problems, like fast acting automatic voltage regulators (AVR) in the generator¹¹, or voltage dependent current order limiters (VDCOL) in HVDC links⁷. In all cases these bifurcations occur on very stressed systems, i.e., the region of stability for the current operating point (stable equilibrium point or s.e.p.) is small, hence, the system is not able to withstand small perturbations and becomes unstable. Although there are reports of these bifurcations occurring in unstressed systems¹², this cannot be considered typical, since power system controls are designed so that eigenvalues of several operating points are well into the left half complex plane.

Some voltage collapse problems can also be associated to voltage control devices like under-load tap changer (ULTC) transformers or AVRs^{13–16}. In some of these cases, but not all, the voltage controls force the eigenvalues to instantaneously jump into the unstable region, making the system immediately unstable. This phenomena is not directly associated to a bifurcation, since the eigenvalues do not go through zero or the imaginary axis. Nevertheless, transcritical bifurcation theory can be used to explain the phenomena when AVR limits are assumed to apply gradually¹⁴.

The particular problem of voltage collapse in power systems has been generally associated with saddle-node bifurcations^{1–8}. These type of instabilities are usually local area voltage problems due to lack of reactive power support, that yield a system wide stability problem characterized by sudden voltage drops.

Saddle-node bifurcations are well defined instabilities in system models fully represented by differential equations^{1, 5, 6, 17, 18}. However, bifurcations in systems that are also modeled with algebraic constraints have just been recently addressed and new results are regularly being reported in the literature^{5, 6, 7, 19}. This paper focuses also on this subject, showing the requirements for having equivalency of typical saddle-node bifurcation conditions between differential equation models and mixed models, i.e., systems represented by both differential equations and algebraic constraints. Furthermore, the paper presents the conditions needed for detecting saddle-node bifurcations in

a proposed ac/dc dynamic system model using only the power flow equations, which are actually a subset of the full steady state equations. This particular issue has been of some concern in power system analysis^{6, 20, 21}.

The numerical robustness of two methods used to detect these type of bifurcations, i.e., direct and parameterized continuation methods, are briefly discussed, since these techniques have been shown to be efficient ways for detecting proximity to voltage collapse²². Finally, a small ac/dc system is used to depict some of the concepts presented in the paper.

II. AC/DC System Model

In this section, a system model is described based on different element models for generators, transmission network, loads, and dc systems. This dynamic model corresponds to a typical representations of ac/dc power systems for voltage and transient stability analysis^{13, 23-29}. Based on this model, it is shown below that a saddle-node bifurcation can be detected using only power flow equations.

Although, long term dynamic elements, such as ULTCs, are not directly considered here, these devices could be easily included without affecting the results presented in this paper for saddle-node bifurcations, as shown for a power flow model in reference 16.

A synchronous generator model with constant terminal voltage and reactive power limits is used, to simulate some of the effects of a voltage regulator^{13, 27}. It is assumed that there are n_G generators, and that the last one is the reference point for the bus voltage phasors. The mechanical power applied to the generator shaft is assumed constant at each load level.

A II-equivalent circuit model is employed to simulated all the elements of the transmission system²⁷. Transformers and phase shifters are included as part of this transmission network.

Voltage and frequency dependent load models are used, since they represent a wide variety of aggregated power system loads^{23, 28, 29}. Hence,

$$\begin{aligned} P_l &= -(P_{l_0} + \Delta P_{l_0} \lambda) - (P_{l_1} + \Delta P_{l_1} \lambda) (V_l/V_l^0)^2 - (P_{l_2} + \Delta P_{l_2} \lambda) (V_l/V_l^0) - D_{l_{f_P}} (\dot{\delta}_l - \omega_{n_G}) - D_{l_{v_P}} \dot{V}_l \\ Q_l &= -(Q_{l_0} + \Delta Q_{l_0} \lambda) - (Q_{l_1} + \Delta Q_{l_1} \lambda) (V_l/V_l^0)^2 - (Q_{l_2} + \Delta Q_{l_2} \lambda) (V_l/V_l^0) - D_{l_{f_Q}} (\dot{\delta}_l - \omega_{n_G}) - D_{l_{v_Q}} \dot{V}_l \end{aligned} \quad (1)$$

where $l = 1 + n_G, 2 + n_G, \dots, n_G + n_L$. Here P_l and Q_l are the powers injected by the load, and $V_l \angle \delta_l$ is the load phasor voltage at bus l . P_{l_0} , P_{l_1} , P_{l_2} , Q_{l_0} , Q_{l_1} , and Q_{l_2} are constant weighting factors that define the steady state base load. $D_{l_{f_P}}$, $D_{l_{v_P}}$, $D_{l_{f_Q}}$, and $D_{l_{v_Q}}$ represent the time constants of the frequency and voltage dependent dynamic terms in seconds. Note that these time constants can be set to zero to represent static load models. ΔP_{l_0} , ΔP_{l_1} , ΔP_{l_2} , ΔQ_{l_0} , ΔQ_{l_1} , ΔQ_{l_2} , and the parameter λ are used to simulate slow time scale load change. For most studies of voltage collapse, it is assumed that the pattern of load change can be represented with one degree of freedom (λ) and that this evolution of load drives the system to a saddle-node bifurcation. The load model presented here allows for a more general analysis of the bifurcating phenomena in power systems, where the load has been shown to have a significant effect in saddle-node bifurcation studies^{22, 30}. Notice that differential equations (1) can be rewritten as

$$\begin{bmatrix} \dot{\delta}_l - \omega_{n_G} \\ \dot{V}_l \end{bmatrix} = \begin{bmatrix} D_{l_{f_P}} & D_{l_{v_P}} \\ D_{l_{f_Q}} & D_{l_{v_Q}} \end{bmatrix}^{-1} \begin{bmatrix} f_{l_\lambda}(\boldsymbol{\delta}, \mathbf{V}) \\ g_{l_\lambda}(\boldsymbol{\delta}, \mathbf{V}) \end{bmatrix}$$

where $f_{l_\lambda}(\boldsymbol{\delta}, \mathbf{V})$ and $g_{l_\lambda}(\boldsymbol{\delta}, \mathbf{V})$ are the active and reactive power mismatches at the load buses, respectively.

It is important to mention that depending on the static load model used to represent the aggregated system loads, the location of a saddle-node bifurcation significantly changes. For example, for a constant PQ load model one can show that the maximum power transfer point, or maximum loadability point, is a saddle-node bifurcation and it also corresponds to the tip the P-V or “nose” curve. This particular issue is discussed at length in reference 8.

DC lines are simulated using R-L circuits, and the HVDC controllers are modeled using saturable PI current controllers with K_P (proportional) and K_I (integral) gains. Although these control circuits are approximations to the more complicated HVDC control structures, they recreate several of the main properties of actual systems, especially when close to the equilibria^{7, 31}. Voltage Dependent Current Order Limiter (VDCOL) can be introduced into this model by representing the controller current order as a nonlinear function of the ac converter voltages^{24, 25}.

The equations that model each element of an ac/dc system can be arranged into vector differential equations (2) below, for an n bus ac/dc system ($n = n_G + n_L + 2n_{dc}$, where n_{dc} is the number of dc links in the system).

The reference generator n_G is assumed to be an infinite bus so that all system equilibria are guaranteed to have $\boldsymbol{\omega}_G = [\omega_1 \dots \omega_{n_G-1}]^T = \mathbf{0}$, otherwise the transfer conductance losses may produce a slight shift in generation frequency at the equilibria for the proposed system model. This condition is not necessary when all generator damping constants are set to zero.

$$\begin{aligned}
\dot{\boldsymbol{\delta}}_G &= \boldsymbol{\omega}_G \\
\mathbf{M}_G \dot{\boldsymbol{\omega}}_G &= \mathbf{f}_G(\boldsymbol{\delta}, \mathbf{V}) - \mathbf{D}_G \boldsymbol{\omega}_G \\
\mathbf{D}_L \begin{bmatrix} \dot{\boldsymbol{\delta}}_L \\ \dot{\mathbf{V}}_L \end{bmatrix} &= \begin{bmatrix} \mathbf{f}_{L\lambda}(\boldsymbol{\delta}, \mathbf{V}) \\ \mathbf{g}_{L\lambda}(\boldsymbol{\delta}, \mathbf{V}) \end{bmatrix} \\
\dot{\mathbf{x}}_{dc} &= \mathbf{h}_{dc}(\mathbf{V}_{dc}, \mathbf{x}_{dc}, \mathbf{y}_{dc}) \\
\mathbf{0} &= \mathbf{G}_\lambda(\boldsymbol{\delta}, \mathbf{V}, \mathbf{x}_{dc}, \mathbf{y}_{dc})
\end{aligned} \tag{2}$$

Vector \mathbf{x}_{dc} stands for all the state variables for the system dc links operating at a fixed control mode, as defined by vector field $\mathbf{h}_{dc}(\cdot)$, so that the dc limit functions are well defined. On the other hand, \mathbf{y}_{dc} represents the dc variables implicitly defined by the corresponding algebraic constraints in $\mathbf{G}(\cdot)$. \mathbf{V} and $\boldsymbol{\delta}$ depict all the voltage phasors at generator ($\mathbf{V}_G \angle \boldsymbol{\delta}_G$), load ($\mathbf{V}_L \angle \boldsymbol{\delta}_L$) and HVDC ($\mathbf{V}_{dc} \angle \boldsymbol{\delta}_{dc}$) buses. Vector functions $\mathbf{f}_G(\cdot)$ and $\mathbf{f}_L(\cdot)$ stand for the active power mismatches at the generator and the load buses, respectively, and $\mathbf{g}_L(\cdot)$ corresponds to the reactive power mismatches at the load buses. Notice that the algebraic constraints represented by the vector field $\mathbf{G}(\cdot)$, correspond to the dc link constraints, the active and/or reactive power mismatches at HVDC and static load buses, and the reactive power equations at all generator buses. Finally, matrices \mathbf{M}_G , \mathbf{D}_G , and \mathbf{D}_L are all nonsingular diagonal or block-diagonal matrices representing the generators' inertia and damping, and the loads' time constants, respectively.

Defining $\mathbf{x} \triangleq [\mathbf{x}_1^T \ \mathbf{x}_2^T]^T$ as some of the state variables associated to the system differential equations, and \mathbf{y} as the system variables associated to the algebraic constraints, equations (2) can be rewritten as

$$\begin{aligned}
\dot{\mathbf{x}}_1 &= \boldsymbol{\omega}_G \\
\underbrace{\begin{bmatrix} \mathbf{M}_G & \mathbf{0} \\ \mathbf{0} & \mathbf{D} \end{bmatrix}}_{\mathbf{K}} \begin{bmatrix} \dot{\boldsymbol{\omega}}_G \\ \dot{\mathbf{x}}_2 \end{bmatrix} &= \begin{bmatrix} \mathbf{F}_{1\lambda}(\mathbf{x}, \mathbf{y}) - \mathbf{D}_G \boldsymbol{\omega}_G \\ \mathbf{F}_{2\lambda}(\mathbf{x}, \mathbf{y}) \end{bmatrix} = \mathbf{F}_\lambda(\boldsymbol{\omega}_G, \mathbf{x}, \mathbf{y}) \\
\mathbf{0} &= \mathbf{G}_\lambda(\mathbf{x}, \mathbf{y})
\end{aligned} \tag{3}$$

where \mathbf{D} is a nonsingular matrix that contains the dynamic load model time constant.

An equilibrium point for equations (3) can be obtained setting the left hand side to zero. Ordinary ac/dc power flow equations correspond to steady state equations $\mathbf{F}_\lambda(\mathbf{0}, \mathbf{x}, \mathbf{y}) = \mathbf{F}_\lambda(\mathbf{x}, \mathbf{y}) = \mathbf{0}$ and $\mathbf{G}_\lambda(\mathbf{x}, \mathbf{y}) = \mathbf{0}$, when the load is modeled as constant PQ. Different static load models could be implemented in the power flow equations, so that these equations can be used to directly determine equilibria of the dynamic model.

For the proposed dynamic system, nonsingularity of the Jacobian $D_y \mathbf{G}(\cdot)$ along system trajectories of interest guarantees a well posed system³² or strictly causal system⁵. If matrix $D_y \mathbf{G}(\cdot)$ becomes singular, then the model represented by (3) breaks down, and dynamic load models should be used then for the system representation. For example, a singular $D_y \mathbf{G}|_0$ at a particular equilibrium point $(\mathbf{0}, \mathbf{x}_0, \mathbf{y}_0, \lambda_0)$ of a simple power system model consisting of one generator, a transmission line and a load, constitutes an impasse point that divides two stable equilibria in a system with no unstable equilibrium points. Although this particular system behavior has been thoroughly analyzed^{19, 33}, it has no physical meaning in a real power network. The same phenomenon was observed in larger ac/dc systems, where two stable equilibria coalesce at a singular Jacobian. In this case, assuming a dynamic voltage dependence of some of the load buses removed the impasse point forcing one of the stable equilibria to become unstable, so that saddle-node theory can be applied to explain the bifurcation in a physical system.

When the algebraic constraints $\mathbf{G}(\cdot)$ have an invertible Jacobian $D_y \mathbf{G}(\cdot)$, variables $\mathbf{y} = \mathbf{h}_\lambda(\mathbf{x})$ can be eliminated (Implicit Function Theorem³⁴), and equations (3) are reduced to

$$\begin{aligned}
\dot{\mathbf{x}}_1 &= \boldsymbol{\omega}_G \\
\mathbf{K} \begin{bmatrix} \dot{\boldsymbol{\omega}}_G \\ \dot{\mathbf{x}}_2 \end{bmatrix} &= \mathbf{F}_\lambda(\boldsymbol{\omega}_G, \mathbf{x}, \mathbf{h}_\lambda(\mathbf{x}))
\end{aligned} \tag{4}$$

which can be rewritten as $\mathbf{M}\dot{\mathbf{z}} = \mathbf{s}_\lambda(\mathbf{z})$, with $\mathbf{z} \triangleq [\mathbf{x}_1^T \ \boldsymbol{\omega}_G^T \ \mathbf{x}_2^T]^T$, and $\mathbf{M} \triangleq \begin{bmatrix} \mathbf{I}_{n_G-1} & \mathbf{0} & \mathbf{0} \\ \mathbf{0} & \mathbf{M}_G & \mathbf{0} \\ \mathbf{0} & \mathbf{0} & \mathbf{D} \end{bmatrix}$.

Notice that, although a variety of operational limits are included in the model, it is assumed throughout this paper that the equations do not change, i.e., the equations and their derivatives are well defined in the vicinity of a saddle-node bifurcation.

III. Equivalency of Saddle-Node Bifurcation Conditions

Some bifurcations, or structural instabilities, for $\mathbf{M}\dot{\mathbf{z}} = \mathbf{s}_\lambda(\mathbf{z})$ occur when the Jacobian $D_z \mathbf{s}(\cdot)$ becomes singular at the equilibrium $(\mathbf{z}_0, \lambda_0)$. Several types of bifurcations characterized by a singular Jacobian are possible, but of these only the saddle-node occurs generically. Moreover, the following conditions apply at the saddle-node¹⁷ $(\mathbf{z}_0, \lambda_0)$:

1. $D_z \mathbf{s}|_0 \triangleq D_z \mathbf{s}_{\lambda_0}(\mathbf{z}_0)$ has a simple and unique zero eigenvalue, with normalized right eigenvector \mathbf{v} and left eigenvector \mathbf{w} , i.e., $D_z \mathbf{s}|_0 \mathbf{v} = \mathbf{0}$ and $\mathbf{w}^T D_z \mathbf{s}|_0 = \mathbf{0}^T$. (5)

2. $\mathbf{w}^T \frac{\partial \mathbf{s}}{\partial \lambda} \Big|_0 \neq 0$. (6)

3. $\mathbf{w}^T [D_z^2 \mathbf{s}|_0 \mathbf{v}] \neq 0$. (7)

Conditions 1 through 3 guarantee the generic quadratic behavior near the bifurcation point, and also prevent singular augmented Jacobians of the Newton- Raphson based methods used to determine bifurcation points as discussed below.

Use of the vector field $\mathbf{s}_\lambda(\mathbf{z})$ in bifurcation analysis of power systems presents several problems, such as the difficulty of finding the explicit function $\mathbf{y} = \mathbf{h}_\lambda(\mathbf{z})$. Typically, function $\mathbf{h}(\cdot)$ cannot be expressed in closed form, though its derivatives are available. While ultimately only the derivatives of $\mathbf{h}(\cdot)$ are needed for computation of the saddle-node bifurcation point, use of the reduced equations sacrifices sparsity, significantly increasing the computational costs. Therefore, it is useful to relate known methods for detecting bifurcations based on saddle-node conditions for the reduced system (4) to conditions expressed in terms of the complete set of system equations (3).

An important computational issue in bifurcation studies for power systems is the relationship between eigenvalues of the Jacobian of the power flow equations*, \mathbf{J}_{PF} , and those of the Jacobian of the system dynamic equations linearized at the equilibrium point, denoted by $\mathbf{J}_{TS} = \mathbf{M}^{-1} D_z \mathbf{s}|_0$. This subject has been studied for a number of ac only system models^{6, 20, 21}. Here it is shown that, for the proposed system model, the power flow equations can be used to directly detect a saddle-node bifurcation of system dynamic equations (4), under the generic assumption of “invertible” algebraic constraints $\mathbf{G}(\cdot)$; moreover, these equations yield information regarding right and left eigenvectors for the linearized equations of the reduce dynamic system (4). These ideas have been briefly discussed for a general dynamic ac system model with no algebraic constraints³⁵.

Thus, the power flow Jacobian at the equilibrium $(\mathbf{0}, \mathbf{x}_0, \mathbf{y}_0, \lambda_0)$ can be represented by

$$\mathbf{J}_{PF} = \left[\begin{array}{cc|c} D_{x_1} \mathbf{F}_1|_0 & D_{x_2} \mathbf{F}_1|_0 & D_y \mathbf{F}_1|_0 \\ D_{x_1} \mathbf{F}_2|_0 & D_{x_2} \mathbf{F}_2|_0 & D_y \mathbf{F}_2|_0 \\ \hline D_{x_1} \mathbf{G}|_0 & D_{x_2} \mathbf{G}|_0 & D_y \mathbf{G}|_0 \end{array} \right]$$

Hence, the determinant of \mathbf{J}_{PF} can be calculated using

$$\det \mathbf{J}_{PF} = \det (D_y \mathbf{G}|_0) \det \left(\left[\begin{array}{cc} D_{x_1} \mathbf{F}_1|_0 & D_{x_2} \mathbf{F}_1|_0 \\ D_{x_1} \mathbf{F}_2|_0 & D_{x_2} \mathbf{F}_2|_0 \end{array} \right] - \left[\begin{array}{c} D_y \mathbf{F}_1|_0 \\ D_y \mathbf{F}_2|_0 \end{array} \right] D_y \mathbf{G}|_0^{-1} \left[\begin{array}{cc} D_{x_1} \mathbf{G}|_0 & D_{x_2} \mathbf{G}|_0 \end{array} \right] \right)$$

On the other hand, linearizing (4) at the equilibrium yields a block Jacobian structure satisfying

$$\mathbf{M} \mathbf{J}_{TS} = \begin{array}{c} \dot{\mathbf{x}}_1 \\ \mathbf{M}_G \dot{\boldsymbol{\omega}}_G \\ \mathbf{D} \dot{\mathbf{x}}_2 \end{array} \boxed{\begin{array}{ccc} \mathbf{x}_1 & \boldsymbol{\omega}_G & \mathbf{x}_2 \\ \mathbf{0} & \mathbf{I}_{n_G-1} & \mathbf{0} \\ D_{x_1} \mathbf{F}_1|_0 + D_y \mathbf{F}_1|_0 D_{x_1} \mathbf{h}|_0 & -\mathbf{D}_G & D_{x_2} \mathbf{F}_1|_0 + D_y \mathbf{F}_1|_0 D_{x_2} \mathbf{h}|_0 \\ D_{x_1} \mathbf{F}_2|_0 + D_y \mathbf{F}_2|_0 D_{x_1} \mathbf{h}|_0 & \mathbf{0} & D_{x_2} \mathbf{F}_2|_0 + D_y \mathbf{F}_2|_0 D_{x_2} \mathbf{h}|_0 \end{array}} \quad (8)$$

Thus, using standard block determinant formulas and since $D_x \mathbf{h}|_0 = -D_y \mathbf{G}|_0^{-1} D_x \mathbf{G}|_0$,

$$\det (D_z \mathbf{s}|_0) = (-1)^k \frac{\det \mathbf{J}_{PF}}{\det (D_y \mathbf{G}|_0)}$$

*The “power flow” equations in this paper differ slightly from the typical set of equations in the power system literature, since static load models used in the simulation are not only constant PQ models.

where k is a positive integer. This equation shows that a singular linearized dynamic equations Jacobian implies having a singular power flow Jacobian, since $\mathbf{G}(\cdot)$ is bounded above. Moreover, theorems 1 and 2 below prove that all saddle-node bifurcation conditions, represented by (5), (6) and (7), have an analogous representation in the power flow equations. In order to simplify the notation, the vector fields $\mathbf{F}(\cdot)$ and $\mathbf{G}(\cdot)$, which represent the power flow equations of the proposed ac/dc system model, are grouped in the vector field $\mathcal{F}(\cdot) \triangleq [\mathbf{F}^T(\cdot) \ \mathbf{G}^T(\cdot)]^T$.

Theorem 1: Let $D_y \mathbf{G}|_0$ be nonsingular at the saddle-node bifurcation point $(\mathbf{0}, \mathbf{x}_0, \mathbf{y}_0, \lambda_0) \in \mathbf{R}^{N+1}$ ($N = 3n_G + 2n_L + 9n_{dc} - 3$) satisfying transversality conditions (5), (6) and (7). Let $\mathcal{F} : \mathbf{R}^{N-n_G+1} \times \mathbf{R} \mapsto \mathbf{R}^{N-n_G+1}$ be as defined above. Hence, for properly normalized left eigenvectors $\mathbf{w} \in \mathbf{R}^m$ (m = number of state variables in (4)) and $\varphi \in \mathbf{R}^{N-n_G+1}$, corresponding to zero eigenvalues of $D_z \mathbf{s}|_0$ and $D_{(x,y)} \mathcal{F}|_0$, respectively, it follows that

$$\mathbf{w}^T \frac{\partial \mathbf{s}}{\partial \lambda} \Big|_0 = \varphi^T \frac{\partial \mathcal{F}}{\partial \lambda} \Big|_0 \quad (9)$$

Furthermore, uniqueness and simplicity of the zero eigenvalue of $D_z \mathbf{s}|_0$ guarantees having a unique eigenvector φ . \square

Proof: Since $D_y \mathbf{G}|_0$ is nonsingular at the equilibrium, there exists a smooth local function $\mathbf{h}(\cdot)$ around $(\mathbf{0}, \mathbf{x}_0, \mathbf{y}_0, \lambda_0)$ such that $\mathbf{y} = \hat{\mathbf{h}}_\lambda(\mathbf{x})$ (Implicit Function Theorem³⁴), and $\partial \mathbf{h} / \partial \lambda|_0 = -D_y \mathbf{G}|_0^{-1} \partial \mathbf{G} / \partial \lambda|_0$. On the other hand, based on the definitions of $\mathbf{s}_\lambda(\mathbf{z})$ and $\mathbf{w} = [\mathbf{w}_{x_1}^T \ \mathbf{w}_{\omega_G}^T \ \mathbf{w}_{x_2}^T]^T$, then $\mathbf{w}^T D_z \mathbf{s}|_0 = \mathbf{0}^T$ implies from (8) that

$$\mathbf{w}_{x_1} = D_G \mathbf{w}_{\omega_G} \quad \text{and} \quad [\mathbf{w}_{\omega_G}^T \ \mathbf{w}_{x_2}^T] (D_x \mathbf{F}|_0 - D_y \mathbf{F}|_0 D_y \mathbf{G}|_0^{-1} D_x \mathbf{G}|_0) = \mathbf{0}^T \quad (10)$$

Now, it follows from $[\varphi_x^T \ \varphi_y^T] D_{(x,y)} \mathcal{F}|_0 = \mathbf{0}^T$ that

$$\varphi_y^T = -\varphi_x^T D_y \mathbf{F}|_0 D_y \mathbf{G}|_0^{-1} \quad \text{and} \quad \varphi_x^T (D_x \mathbf{F}|_0 - D_y \mathbf{F}|_0 D_y \mathbf{G}|_0^{-1} D_x \mathbf{G}|_0) = \mathbf{0}^T \quad (11)$$

For properly scaled eigenvectors, from (10) and (11), and since \mathbf{w} is unique by definition, one has a unique eigenvector $\varphi = [\varphi_x^T \ \varphi_y^T]^T$, with $\varphi_x = [\mathbf{w}_{\omega_G}^T \ \mathbf{w}_{x_2}^T]^T$. Furthermore,

$$\begin{aligned} \mathbf{w}^T \frac{\partial \mathbf{s}}{\partial \lambda} \Big|_0 &= [\mathbf{w}_{\omega_G}^T \ \mathbf{w}_{x_2}^T] \left(\frac{\partial \mathbf{F}}{\partial \lambda} \Big|_0 - D_y \mathbf{F}|_0 D_y \mathbf{G}|_0^{-1} \frac{\partial \mathbf{G}}{\partial \lambda} \Big|_0 \right) \\ &= \varphi_x^T \frac{\partial \mathbf{F}}{\partial \lambda} \Big|_0 - \varphi_x^T D_y \mathbf{F}|_0 D_y \mathbf{G}|_0^{-1} \frac{\partial \mathbf{G}}{\partial \lambda} \Big|_0 = \varphi^T \frac{\partial \mathcal{F}}{\partial \lambda} \Big|_0 \end{aligned}$$

Theorem 2: Let $D_y \hat{\mathbf{G}}|_0$ be nonsingular at the saddle-node bifurcation point $(\mathbf{0}, \mathbf{x}_0, \mathbf{y}_0, \lambda_0) \in \mathbf{R}^{N+1}$ satisfying transversality conditions (5), (6) and (7). Let $\mathcal{F}(\cdot)$, \mathbf{w} , and φ be defined as in theorem 1. Then, for properly normalized right eigenvectors $\mathbf{v} \in \mathbf{R}^m$ and $\mathbf{v} \in \mathbf{R}^{N-n_G+1}$, corresponding to zero eigenvalues of $D_z \mathbf{s}|_0$ and $D_{(x,y)} \mathcal{F}|_0$, respectively, i.e., $D_z \mathbf{s}|_0 \mathbf{v} = \mathbf{0}$, and $D_{(x,y)} \mathcal{F}|_0 \mathbf{v} = \mathbf{0}$, it follows that

$$\mathbf{w}^T [D_z^2 \mathbf{s}|_0 \mathbf{v}] \mathbf{v} = \varphi^T [D_{(x,y)}^2 \mathcal{F}|_0 \mathbf{v}] \mathbf{v} \quad (12)$$

Proof: Following similar arguments to the ones employed in the proof of theorem 1, one has that for $\mathbf{v} = [\mathbf{v}_{x_1}^T \ \mathbf{v}_{\omega_G}^T \ \mathbf{v}_{x_2}^T]^T$ and $\mathbf{v} = [\mathbf{v}_x^T \ \mathbf{v}_y^T]^T$, $\mathbf{v}_{\omega_G} = \mathbf{0}$, $\mathbf{v}_y = -D_y \mathbf{G}|_0^{-1} D_x \mathbf{G}|_0 \mathbf{v}_x$, and $\mathbf{v}_x = [\mathbf{v}_{x_1}^T \ \mathbf{v}_{x_2}^T]^T \triangleq \mathbf{v}_x$. Furthermore, the product of the tensor $D_{(x,y)}^2 \mathcal{F}|_0$ and the vector \mathbf{v} , yields the matrix

$$D_{(x,y)}^2 \mathcal{F}|_0 \mathbf{v} = \begin{bmatrix} D_x^2 \mathbf{F}|_0 \mathbf{v}_x - D_{xy}^2 \mathbf{F}|_0 D_y \mathbf{G}|_0^{-1} D_x \mathbf{G}|_0 \mathbf{v}_x & D_{yx}^2 \mathbf{F}|_0 \mathbf{v}_x - D_y^2 \mathbf{F}|_0 D_y \mathbf{G}|_0^{-1} D_x \mathbf{G}|_0 \mathbf{v}_x \\ D_x^2 \mathbf{G}|_0 \mathbf{v}_x - D_{xy}^2 \mathbf{G}|_0 D_y \mathbf{G}|_0^{-1} D_x \mathbf{G}|_0 \mathbf{v}_x & D_{yx}^2 \mathbf{G}|_0 \mathbf{v}_x - D_y^2 \mathbf{G}|_0 D_y \mathbf{G}|_0^{-1} D_x \mathbf{G}|_0 \mathbf{v}_x \end{bmatrix}$$

Hence, it can be shown that

$$\begin{aligned} \varphi^T [D_{(x,y)}^2 \mathcal{F}|_0 \mathbf{v}] \mathbf{v} &= \varphi_x^T [D_x^2 \mathbf{F}|_0 \mathbf{v}_x - D_{xy}^2 \mathbf{F}|_0 D_y \mathbf{G}|_0^{-1} D_x \mathbf{G}|_0 \mathbf{v}_x - D_{yx}^2 \mathbf{F}|_0 \mathbf{v}_x D_y \mathbf{G}|_0^{-1} D_x \mathbf{G}|_0 + \\ &D_y^2 \mathbf{F}|_0 D_y \mathbf{G}|_0^{-1} D_x \mathbf{G}|_0 \mathbf{v}_x D_y \mathbf{G}|_0^{-1} D_x \mathbf{G}|_0 - D_y \mathbf{F}|_0 D_y \mathbf{G}|_0^{-1} D_x^2 \mathbf{G}|_0 \mathbf{v}_x + \\ &D_y \mathbf{F}|_0 D_y \mathbf{G}|_0^{-1} D_{xy}^2 \mathbf{G}|_0 D_y \mathbf{G}|_0^{-1} D_x \mathbf{G}|_0 \mathbf{v}_x + D_y \mathbf{F}|_0 D_y \mathbf{G}|_0^{-1} D_{yx}^2 \mathbf{G}|_0 \mathbf{v}_x D_y \mathbf{G}|_0^{-1} D_x \mathbf{G}|_0 - \\ &D_y \mathbf{F}|_0 D_y \mathbf{G}|_0^{-1} D_y^2 \mathbf{G}|_0 D_y \mathbf{G}|_0^{-1} D_x \mathbf{G}|_0 \mathbf{v}_x D_y \mathbf{G}|_0^{-1} D_x \mathbf{G}|_0] \mathbf{v}_x \end{aligned} \quad (13)$$

On the other hand, since in a neighborhood of the bifurcation point the Implicit Function theorem implies that $\mathbf{y} = \mathbf{h}_\lambda(\mathbf{x})$, then

$$[D_z^2 \mathbf{s}|_0 \mathbf{v}] \mathbf{v} = \begin{bmatrix} \mathbf{0} \\ (D_x^2 \mathbf{F}|_0 \mathbf{v}_x + D_{yx}^2 \mathbf{F}|_0 \mathbf{v}_x D_x \mathbf{h}|_0 + D_{xy}^2 \mathbf{F}|_0 D_x \mathbf{h}|_0 \mathbf{v}_x + D_y^2 \mathbf{F}|_0 D_x \mathbf{h}|_0 \mathbf{v}_x D_x \mathbf{h}|_0 + D_y \mathbf{F}|_0 D_x \mathbf{p}|_0) \mathbf{v}_x \end{bmatrix} \quad (14)$$

where $\mathbf{p}_\lambda(\mathbf{x}) \triangleq D_x \mathbf{h}_\lambda(\mathbf{x}) \mathbf{v}_x$. Now, since $D_x \mathbf{h}|_0 = -D_y \mathbf{G}|_0^{-1} D_x \mathbf{G}|_0$, it can be shown that

$$D_x \mathbf{p}|_0 = -D_y \mathbf{G}|_0^{-1} [D_x^2 \mathbf{G}|_0 \mathbf{v}_x + D_{yx}^2 \mathbf{G}|_0 \mathbf{v}_x D_x \mathbf{h}|_0 + D_{xy}^2 \mathbf{G}|_0 D_x \mathbf{h}|_0 \mathbf{v}_x + D_y^2 \mathbf{G}|_0 D_x \mathbf{h}|_0 \mathbf{v}_x D_x \mathbf{h}|_0] \quad (15)$$

Therefore, from (13), (14) and (15), it follows that $\mathbf{w}^T [D_z^2 \mathbf{s}|_0 \mathbf{v}] \mathbf{v} = \boldsymbol{\varphi}^T [D_{(x,y)}^2 \mathcal{F}|_0 \mathbf{v}] \mathbf{v}$ \square

As shown in the previous theorems, the left and right eigenvectors $\boldsymbol{\varphi}$ and \mathbf{v} , respectively, obtained from the power flow equations, contain the information of the dynamic equations eigenvectors at the bifurcation point, i.e., \mathbf{w} and \mathbf{v} . Right eigenvectors are used to determine how the bifurcation occurs¹, and yield information regarding the areas in the power network prone to having voltage problems^{10, 16, 22}. Left eigenvectors are used to determine corrective measures to improve voltage stability³⁶, and also can be used to determine the closest saddle-node bifurcation in parameter space³⁷.

IV. Detecting Bifurcations

There are several well known techniques for detecting bifurcations in dynamic systems¹⁸. However, in power system analysis two methods, namely, direct (Point of Collapse or PoC) and continuation methods, have been successfully used to detect saddle-node bifurcations in a variety of network models^{7, 16, 38-43}. One of the main concerns when applying these methods is the singularity of the corresponding equations' Jacobians at the bifurcation point, which could cause numerical problems when a Newton-Raphson solution algorithm is used. In this section, the nonsingularity of the Jacobians at a saddle-node bifurcation point for both methods are briefly discussed.

IV.1. Direct Methods

Using $\mathcal{F}(\cdot)$ and $\boldsymbol{\varphi}$ as defined above, and defining $\boldsymbol{\chi} \triangleq [\mathbf{x}^T \ \mathbf{y}^T]^T$, the left eigenvector PoC equations can be written as

$$\begin{aligned} D_\chi \mathcal{F}_\lambda(\boldsymbol{\chi})^T \boldsymbol{\varphi} &= \mathbf{0} \\ \mathcal{F}_\lambda(\boldsymbol{\chi}) &= \mathbf{0} \\ \frac{\partial \mathcal{F}_\lambda(\boldsymbol{\chi})^T}{\partial \lambda} \boldsymbol{\varphi} &= k \end{aligned} \quad \Rightarrow \quad \mathbf{J}_{PoC} = \begin{bmatrix} D_\chi^2 \mathcal{F}|_0^T \boldsymbol{\varphi} & D_\chi \mathcal{F}|_0^T & D_{\lambda\chi} \mathcal{F}|_0^T \boldsymbol{\varphi} \\ D_\chi \mathcal{F}|_0 & \mathbf{0} & \frac{\partial \mathcal{F}}{\partial \lambda}|_0 \\ \boldsymbol{\varphi}^T D_{\chi\lambda} \mathcal{F}|_0 & \frac{\partial \mathcal{F}}{\partial \lambda}|_0^T & \boldsymbol{\varphi}^T \frac{\partial^2 \mathcal{F}}{\partial \lambda^2}|_0 \end{bmatrix}$$

Where k is any scalar different from zero. In spite of the individual block $D_\chi \mathcal{F}|_0$ being singular in the Jacobian \mathbf{J}_{PoC} , conditions (6) and (7), together with the nonsingularity of $D_y \mathbf{G}|_0$, guarantee that \mathbf{J}_{PoC} is nonsingular^{44, 45}.

Similar arguments can be used to formally prove nonsingularity of the Jacobians corresponding to the alternate PoC equations (16) shown below. These equations have proven to be computationally more efficient than (16)¹⁶.

$$\begin{aligned} D_\chi \mathcal{F}_\lambda(\boldsymbol{\chi}) \mathbf{v} &= \mathbf{0} & D_\chi \mathcal{F}_\lambda(\boldsymbol{\chi})^T \boldsymbol{\varphi} &= \mathbf{0} \\ \mathcal{F}_\lambda(\boldsymbol{\chi}) &= \mathbf{0} & \mathcal{F}_\lambda(\boldsymbol{\chi}) &= \mathbf{0} \\ \|\mathbf{v}\|_\infty &= 1 & \|\boldsymbol{\varphi}\|_\infty &= 1 \end{aligned} \quad (16)$$

IV.2. Continuation Methods

Continuation methods have been used since the 60's in a variety of engineering fields¹⁸. Parameterization and perpendicular intersection techniques can be used to trace the branch of equilibria associated to saddle-node bifurcations in ac/dc networks¹⁶. This parameterized continuation method consists of a three step approach, namely, prediction, correction, and parameterization, to tracing the equilibrium points as one parameter in the system changes, i.e., find the solutions to the steady state equations $\mathbf{s}_\lambda(\mathbf{z}) = \mathbf{0}$, for a given set of parameter values. Typically, the loading factor λ is the varying parameter; however, as the system gets closer to bifurcation, the Jacobian $D_z \mathbf{s}|_0$ becomes ill-conditioned. Thus, a change of parameter (parameterization step), such as switching from λ to a state variable $z_i \in \mathbf{z}$, makes the Jacobian nonsingular⁴⁴.

For the power system dynamic model used throughout this paper, where the power flow equations are represented by the vector field $\mathcal{F}(\cdot)$, and for a nonsingular Jacobian $D_y \mathbf{G}|_0$, there is a one to one correspondence between the equilibria of $\mathbf{s}(\cdot)$ and the solutions of $\mathcal{F}_\lambda(\boldsymbol{\chi}) = \mathbf{0}$. Furthermore, based on theorems 1 and 2, a saddle-node bifurcation in the vector field $\mathbf{s}(\cdot)$ can be detected using $\mathcal{F}(\cdot)$. Therefore, one can trace a bifurcation branch utilizing the power flow equations in the continuation method¹⁶, with predictor and corrector steps having nonsingular Jacobians⁴⁴.

V. Example

The ac/dc system in Figure 1 was used to depict some of ideas discussed in the paper. Tables 1 through 3 show the steady state and dynamic data for the system. The load at bus 2 is modeled as a frequency dependent active power plus a voltage dependent reactive power term, i.e.,

$$\begin{aligned} P_l &= P_{l_0} + dP + D_l \delta_2 \\ Q_l &= \left(\frac{V_2}{V_{2_0}} \right)^2 Q_{l_0} \end{aligned}$$

where $P_{l_0} = 4.75$, $Q_{l_0} = 1.561$, $D_l = 0.1$, and $V_{2_0} = 1.01965$, all in p.u. The active power load change at bus 2 is chosen as the slowly changing system parameter, i.e., $\lambda = dP$. The infinite bus absorbs all losses and load power changes in the system.

Figures 2 and 3 depict part of the bifurcation diagrams, PV or “nose” curves, for the rectifier and inverter ac voltages when the parameter dP changes, and were obtained using a continuation method. These diagrams were traced up to the maximum value of dP , or maximum loading point, which corresponds to a saddle-node bifurcation. The continuous line represents the stable equilibrium points, whereas the dashed line depicts the unstable equilibrium points. Not all unstable equilibrium points were traced, since they are not relevant to this paper. Notice that in Figure 2, the system is stable up to the saddle-node bifurcation, whereas in Figure 3 the system loses stability at $dP = 46.82$ p.u. due to a Hopf bifurcation induced by the VDCOL.

In this example, the number of state variables \mathbf{z} is 7 and of algebraic variables \mathbf{y} is 10, whereas the number of power flow variables $\boldsymbol{\chi}$ is 15. By tracing the eigenvalues of the dynamic Jacobian $J_{TS(\tau \times \tau)}$ and the power flow Jacobian $J_{PF(15 \times 15)}$, for all the equilibrium points depicted in Figures 2 and 3, one can observe that both become singular at the maximum loading point, as expected. However, the Hopf bifurcation depicted in Figure 3 can only be detected using J_{TS} . On the other hand, the direct method can only be applied in practice to the power flow equations, since a symbolic J_{TS} is actually needed to set up the problem, and obtaining this set of equations takes several days in a workstation (using MapleV in a dedicated 32MB-RAM SPARCstation-LX with 200MB swap space), whereas getting J_{PF} takes only a couple of seconds. The direct method yields $dP_{max} = 44.66$ p.u. for the system without VDCOL, and $dP_{max} = 46.84$ p.u. with VDCOL.

VI. Conclusions

This paper discusses the conditions needed for detecting saddle-node bifurcations using power flow equations, for a differential equation and algebraic constraint model of an ac/dc power system. The algebraic equations’ Jacobian must be nonsingular along system trajectories of interest to have a well posed physical dynamic system. Hence, the paper shows that the power flow equations meet the same conditions at a saddle-node bifurcation point as the reduced differential equations, which are formed by eliminating the algebraic constraints in the model. The paper demonstrates that a more complete static load model in the power flow equations suffices for detecting bifurcation points of the proposed system model by means of these static equations. Furthermore, the similarities of the eigenvectors at the saddle-node bifurcation between the power flow and the reduced dynamic equations, yield important information regarding the characteristics of the system at the bifurcation point, so that control actions can be taken to improve voltage stability throughout the system.

The equivalency of saddle-node bifurcation conditions between the differential equations model and the power flow equations, can then be used to prove that direct and parameterized continuation methods have nonsingular Jacobians at saddle-node bifurcation points, which makes these techniques powerful computational tools for measuring proximity to points of collapse.

VII. Acknowledgment

The author would like to thank Professors Ian Dobson and Christopher L. DeMarco from the Department of Electrical and Computer Engineering at the University of Wisconsin, for their comments and suggestions.

VIII. References

- 1 **Dobson, I and Chiang, H D** ‘Towards a Theory of Voltage Collapse in Electric Power Systems’ *Systems & Control Letters* 13 (1989) pp 253–262
- 2 **Begovic, M M and Phadke, A G** ‘Dynamic Simulation of Voltage Collapse’ *IEEE Trans. Power Systems* Vol 5 No 1 (February 1990) pp 198–203
- 3 **Fink, L H** ed *Proceedings: Bulk Power System Voltage Phenomena—Voltage Stability and Security* EPRI EL-6183 (January 1989)
- 4 **Fink, L H** ed *Proceedings: Bulk Power System Voltage Phenomena—Voltage Stability and Security* ECC/NSF Workshop, Fairfax, VA, Ecc Inc (August 1991)
- 5 **Kwatny, H G, Pasrija, A K and Bahar, L Y** ‘Static Bifurcations in Electric Power Networks: Loss of Steady-State Stability and Voltage Collapse’ *IEEE Trans. on Circuits and Syst* Vol 33 No 10 (October 1986) pp 981–991
- 6 **Kwatny, H G** ‘Steady State Analysis of Voltage Instability Phenomena’ in reference 3 pp 51–522
- 7 **Cañizares, C A, Alvarado, F L, DeMarco, C L, Dobson, I and Long, W F** ‘Point of Collapse Methods Applied to AC/DC Power Systems’ *IEEE Trans. Power Systems* Vol 7 No 2 (May 1992) pp 673–683
- 8 **Cañizares, C A** ‘On Bifurcations, Voltage Collapse and Load Modelling’ accepted for publication in the *IEEE Trans. Power Systems* (1994).
- 9 **Ajjarapu, V and Lee, B** ‘Bifurcation Theory and its Application to Nonlinear Dynamical Phenomena in an Electrical Power System’ *IEEE Trans. Power Systems* Vol 7 No 2 (February 1992) pp 424–431
- 10 **Gao, B, Morison, G K and Kundur, P** ‘Voltage Stability Evaluation Using Modal Analysis’ *IEEE Trans. Power Systems* Vol 7 No 4 (November 1992) pp 1529–1542
- 11 **Abed, E H and Varaiya, P P** ‘Nonlinear Oscillations in Power Systems’ *International Journal of Electric Power & Energy Systems* Vol 6 (1984) pp 37–43
- 12 **Sauer, P W, Lesieutre, B C, and Pai, M A** ‘Dynamic vs. Static Aspects of Voltage Problems’ in reference 4 pp 207–216
- 13 **Liu, C-C and Vu, K** ‘Type of Voltage Collapse Problems’ in reference 4 pp 133–141
- 14 **Dobson, I and Lu, L** ‘Voltage Collapse Precipitated by the Immediate Change in Stability When Generator Reactive Power Limits are Encountered’ *IEEE Trans. Circuits and Syst.-I* Vol 39 No 9 (September 1992) pp 762–766
- 15 **Morrison, G K, Gao, B and Kundur, P** ‘Voltage Stability Analysis Using Static and Dynamic Approaches’ *IEEE Trans. Power Systems* Vol 8 No 3 (August 1993) pp 1159–1171
- 16 **Cañizares, C A and Alvarado, F L** ‘Point of Collapse and Continuation Methods for Large AC/DC Systems’ *IEEE Trans. Power Systems* Vol 8 No 1 (February 1993) pp 1–8
- 17 **Guckenheimer, J and Holmes, P** *Nonlinear Oscillations Dynamical Systems and Bifurcations of Vector Fields* Springer-Verlag, New York (1986)
- 18 **Seydel, R** *From Equilibrium to Chaos—Practical Bifurcation and Stability Analysis* Elsevier Science Publishers, North-Holland (1988)
- 19 **Guo, T and Schlueter, R A** ‘Identification of Generic Bifurcation and Stability Problems in Power System Differential-Algebraic Models’ *IEEE-PES Summer Meeting* Vancouver, BC (July 1993) paper 93 SM 513–2 PWRS
- 20 **Sastry, S and Variaya, P P** ‘Hierarchical Stability and Alert State Steering Control of Interconnected Power Systems’ *IEEE Trans. Circuits and Syst.* Vol 27 No 11 (November 1980) pp 1102–1112
- 21 **Sauer, P W and Pai, M A** ‘Power System Steady-State Stability and the Load Flow Jacobian’ *IEEE Trans. Power Systems* Vol 5 No 4 (November 1990) pp 1374–1383
- 22 **Cañizares, C A, Long, W F, Alvarado, F L and DeMarco, C L** ‘Techniques for Detecting Proximity to Voltage Collapse in AC/DC Systems’ *Proc. III SEPOPE* Belo Horizonte, Brazil (May 1992) paper IP-18
- 23 *Extended Transient–Midterm Stability Package: Final Report* EPRI EL-4610 (January 1987)
- 24 *Methodology of Integration of HVDC Links in Large AC Systems—Phase 1: Reference Manual* EPRI EL-3004 (March 1983)

- 25 *Methodology of Integration of HVDC Links in Large AC Systems—Phase 2: Advanced Concepts* EPRI EL-4365 Vol 1 (April 1987)
- 26 **Arrillaga, J** *High Voltage Direct Current Transmission* Peter Peregrinus London, UK (1983)
- 27 **Arrillaga, J, Arnold, C P and Harker, B J** *Computer Modelling of Electrical Power Systems* John Wiley & Sons, UK (1983)
- 28 **Walve, K** ‘Modelling of Power System Components at Severe Disturbances’ *CIGRE Int. Conf. Large High Voltage Electric Syst.* (August 1986) paper 38-18
- 29 **Jimma, K, Tomac, A, Vu, K and Liu, C-C** ‘A Study of Dynamic Load Models for Voltage Collapse Analysis’ in reference 4 pp 423–429
- 30 **Pal, M K** ‘Voltage Stability Conditions Considering Load Characteristics’ *IEEE Trans. Power Systems* Vol 7 No 1 (February 1992) pp 243–249
- 31 **DeMarco, C L and Cañizares, C A** ‘A Vector Energy Function Approach for Security Analysis of AC/DC Systems’ *IEEE Trans. Power Systems* Vol 7 No 3 (August 1992) pp 1001–1011
- 32 **DeMarco, C L and Bergen, A R** ‘Application of Singular Perturbation Techniques to Power System Transient Stability Analysis’ *Proc. ISCAS* (May 1984) pp 597–601
- 33 **Venkatasubramanian, V, Schättler, H and Zaborszky, J** ‘A Taxonomy of the Dynamics of the Large Power System with Emphasis on its Voltage Stability’ in reference 4 pp 9–52
- 34 **Rudin, W** *Principles of Mathematical Analysis* Third Edition McGraw-Hill, USA (1976)
- 35 **Dobson, I** ‘Observations on the Geometry of Saddle Node Bifurcations and Voltage Collapse in Electrical Power Systems’ *IEEE Trans. Circuits and Syst.-I: Fund. Theory and App.* Vol 39 No 3 (March 1992) pp 240–243
- 36 **Dobson, I and Lu, L** ‘Computing an Optimum Direction in Control Space to Avoid Saddle Node Bifurcation and Voltage Collapse in Electric Power Systems’ *IEEE Trans. Automatic Control* Vol 37 No 10 (October 1992) pp 1616–1620
- 37 **Dobson, I and Lu, L** ‘New methods for computing a closest saddle node bifurcation and worst case load power margin for voltage collapse’ *IEEE-PES Summer Meeting* Seattle, WA (July 1992) paper 92 SM 587–6 PWRS
- 38 **Alvarado, F L and Jung, T H** ‘Direct Detection of Voltage Collapse Conditions’ in reference 3 pp 523–538
- 39 **Ajjarapu, V** ‘Identification of Steady-State Voltage Stability in Power Systems’ *IASTED Proc. Int. Conf. High Tech. in the Power Industry* Phoenix, Arizona (March 1988) pp 244–247
- 40 **Van Cutsem, T** ‘A Method to Compute Reactive Power Margins with respect to Voltage Collapse’ *IEEE Trans. Power Systems* Vol 6 No 2 (February 1991) pp 145–156
- 41 **Chiang, H D, Ma, W, Thoma, R J and Thorp, J S** ‘Tools for Analyzing Voltage Collapse in Electric Power Systems’ *Proc. Tenth Power System Computation Conf* Graz, Austria (August 1990) pp 1210–1217
- 42 **Iba, K, Suzuki, H, Egawa, M and Watanabe, T** ‘Calculation of Critical Loading Condition with Nose Curve Using Homotopy Continuation Method’ *IEEE Trans. Power Systems* Vol 6 No 2 (May 1991) pp 584–593
- 43 **Ajjarapu, V and Christy, C** ‘The Continuation Power Flow: A Tool for Steady State Voltage Stability analysis’ *IEEE PICA Conference Proc.* (May 1991) pp 304–311
- 44 **Cañizares, C A** ‘Saddle-Node Bifurcations in Power Systems’ *Jornadas de Ingeniería Eléctrica y Electrónica* Quito, Ecuador (July 1993) pp 222–229
- 45 **Spence, A and Werner, B** ‘Non-simple Turning Points and Cusps’ *IMA Journal of Numerical Analysis* No 2 (1982) pp 413–427

Table 1: AC transmission system data in p.u. for a 550 kV and 100 MVA base.

Element	G	B	$-B_s$
Line 1-2	3.68	54.13	4.68
Line 2-3	3.68	54.13	4.68
Transf. G_1		166.67	
Transf. G_2		100.00	
Transf. ∞		100.00	
Capac. 1			13.00
Capac. 3			13.68

Table 2: Generator data in p.u.

Generator	Inertia M	Damping D	Terminal Voltage V_t	Mechanical Power P_m
G_1	0.1	0.001	1	40
G_2	0.016	0.001	1	4.75
∞	∞	0	1	—

Table 3: DC system data in p.u. for a 550 kV and 2.5 kA base.

Variable	Rectifier	Inverter
K_P	1	1
K_I	75	75
Commutation reactance X_c	0.1345	0.1257
Tap a	1.7634	1.7678
Min. firing angle α_{min}	5^0	$\sim 120^{0\dagger}$
Max. firing angle α_{max}	120^0	$\sim 142^{0\dagger}$
Min. extinction angle γ_{min}	$\sim 40^{0\dagger}$	18^0
Max. extinction angle γ_{max}	$\sim 155^{0\dagger}$	40^0
Current order I_o	1.0	0.9
Min. current order $I_{o_{min}}^\ddagger$	0.1	0.0
Max. ac voltage $V_{ac_{max}}^\ddagger$	0.95	0.95
Min. ac voltage $V_{ac_{min}}^\ddagger$	0.5	0.5
DC resistance R_d	0.0624	

† Assuming $\mu \approx 20^0$

‡ VDCOL

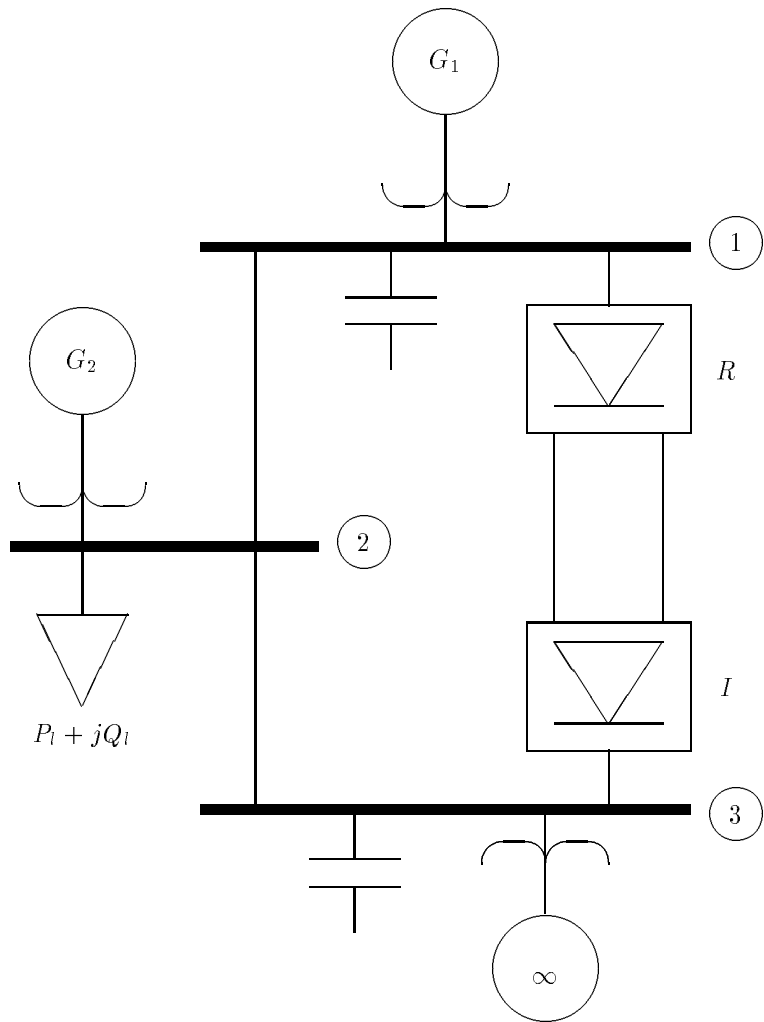


Figure 1: Sample ac/dc system

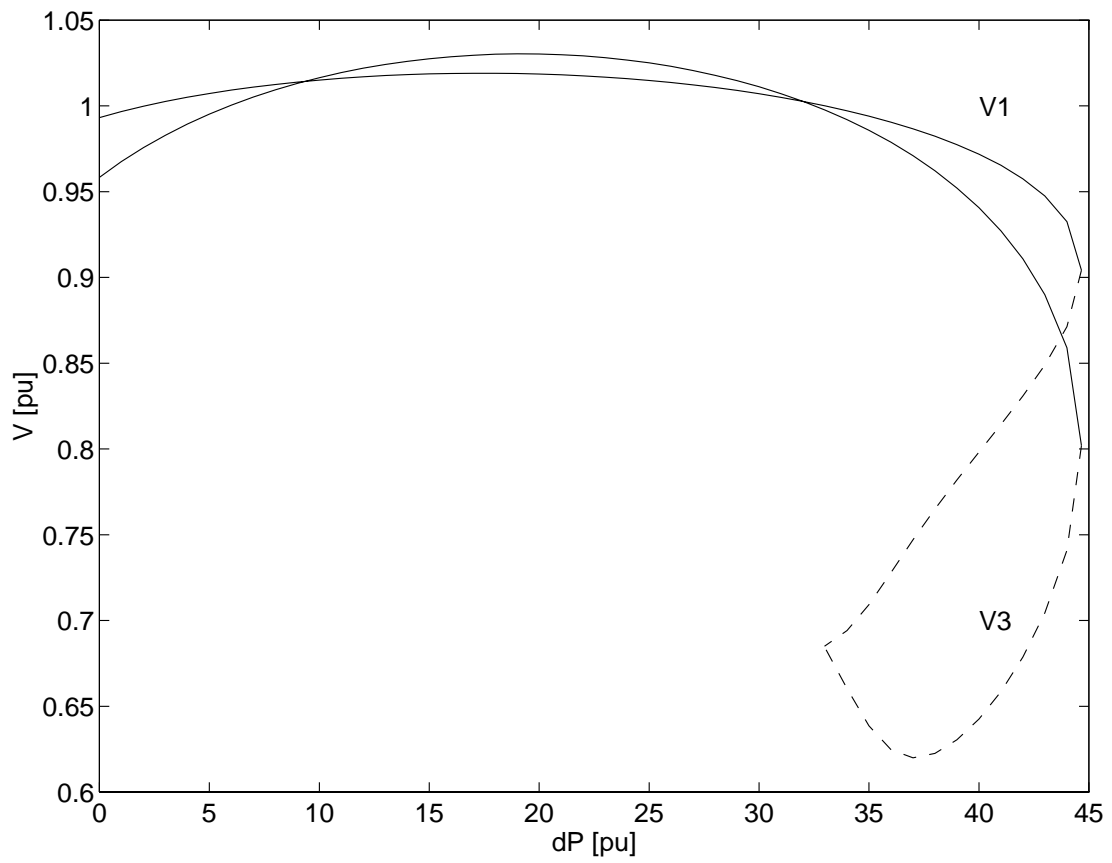


Figure 2: Bifurcation diagram for ac/dc system with *no* VDCOL.

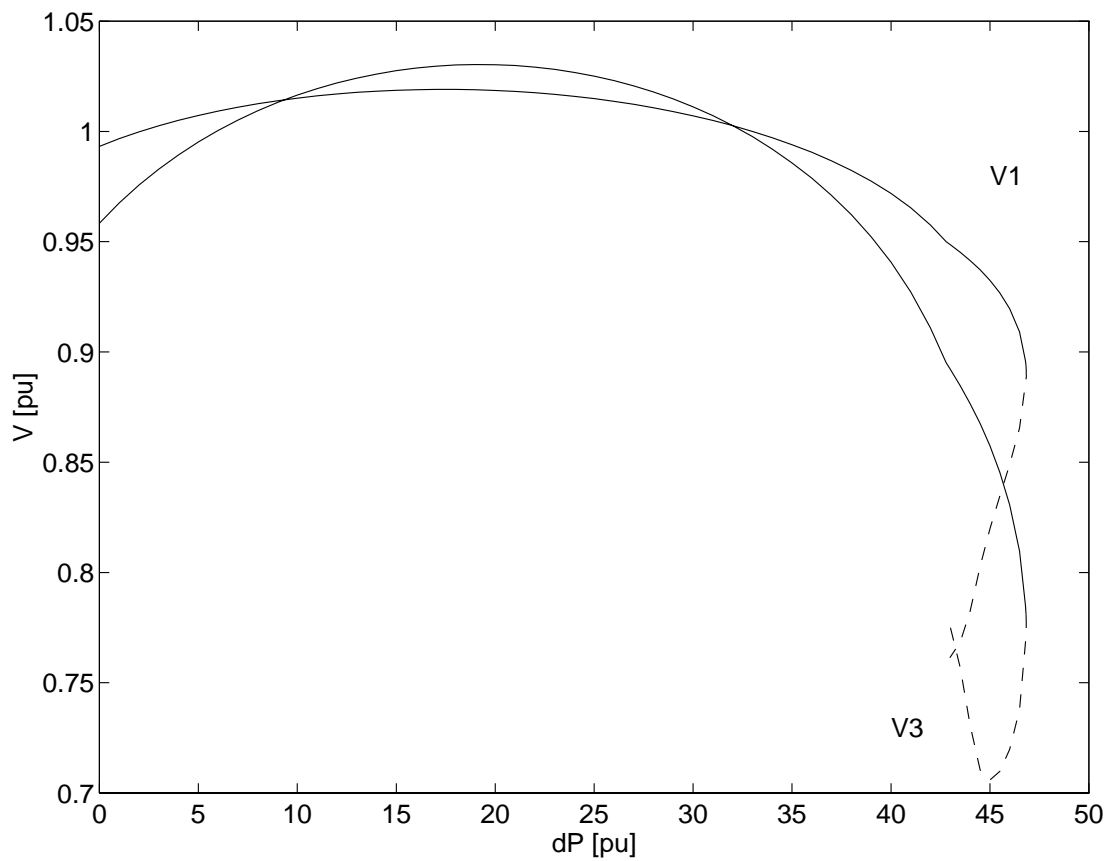


Figure 3: Bifurcation diagram for ac/dc system with VDCOL. The system becomes unstable at $dP = 46.82\text{p.u.}$ due to a Hopf bifurcation ($dP_{max} = 46.84\text{p.u.}$).